


Solar cell efficiency tables (version 59)

Martin A. Green¹  | Ewan D. Dunlop² | Jochen Hohl-Ebinger³ |
Masahiro Yoshita⁴ | Nikos Kopidakis⁵ | Xiaojing Hao¹

¹Australian Centre for Advanced Photovoltaics, School of Photovoltaic and Renewable Energy Engineering, University of New South Wales, Sydney, New South Wales, Australia

²Directorate C–Energy, Transport and Climate, European Commission–Joint Research Centre, Ispra, Italy

³Department of Characterisation and Simulation/CalLab Cells, Fraunhofer-Institute for Solar Energy Systems, Freiburg, Germany

⁴Renewable Energy Research Center (RENRC), National Institute of Advanced Industrial Science and Technology (AIST), Ibaraki, Japan

⁵National Renewable Energy Laboratory, Golden, Colorado, USA

Correspondence

Martin A. Green, School of Photovoltaic and Renewable Energy Engineering, University of New South Wales, Sydney, 2052, New South Wales, Australia.

Email: m.green@unsw.edu.au

Funding information

New Energy and Industrial Technology Development Organization; U.S. Department of Energy (Office of Science, Office of Basic Energy Sciences and Energy Efficiency and Renewable Energy, Solar Energy Technology Program); Australian Renewable Energy Agency

Abstract

Consolidated tables showing an extensive listing of the highest independently confirmed efficiencies for solar cells and modules are presented. Guidelines for inclusion of results into these tables are outlined, and new entries since June 2021 are reviewed.

KEYWORDS

energy conversion efficiency, photovoltaic efficiency, solar cell efficiency

1 | INTRODUCTION

Since January 1993, “*Progress in Photovoltaics*” has published six monthly listings of the highest confirmed efficiencies for a range of photovoltaic cell and module technologies.^{1–3} By providing guidelines for inclusion of results into these tables, this not only provides an authoritative summary of the current state-of-the-art but also encourages researchers to seek independent confirmation of results and to report results on a standardized basis. In Version 33 of these tables,² results were updated to the new internationally accepted reference spectrum (International Electrotechnical Commission IEC 60904-3, Ed. 2, 2008).

The most important criterion for inclusion of results into the tables is that they must have been independently measured by a recognized test center listed in an earlier issue³ (also see Appendix A). A distinction is made between three different eligible definitions of cell area: total area, aperture area and designated illumination area, as defined in an earlier issue³ (note that, if masking is used, masks must have a simple aperture geometry, such as square, rectangular or circular). “Active area” efficiencies are not included. There are also certain minimum values of the area sought for the different device types (above 0.05 cm² for a concentrator cell, 1 cm² for a one-sun cell, 800 cm² for a module and 200-cm² for a “submodule”).

TABLE 1 Confirmed single-junction terrestrial cell and submodule efficiencies measured under the global AM1.5 spectrum (1000 W/m²) at 25°C (IEC 60904-3: 2008 or ASTM G-173-03 global)

Classification	Efficiency (%)	Area (cm ²)	V _{oc} (V)	J _{sc} (mA/cm ²)	Fill factor (%)	Test center (date)	Description
<i>Silicon</i>							
Si (crystalline cell)	26.7 ± 0.5	79.0 (da)	0.738	42.65 ^a	84.9	AIST (3/17)	Kaneka, n-type rear IBC ¹⁰
Si (crystalline cell)	26.3 ± 0.4	274.3 (t)	0.7502	40.49 ^b	86.6	ISFH (9/21)	LONGi, n-type HJT ⁴
Si (DS wafer cell)	24.4 ± 0.3	267.5 (t)	0.7132	41.47 ^{d,e}	82.5	ISFH (8/20)	Jinko Solar, n-type
Si (thin transfer submodule)	21.2 ± 0.4	239.7 (ap)	0.687 ^c	38.50 ^{d,e}	80.3	NREL (4/14)	Solexel (35 μm thick) ¹¹
Si (thin film minimodule)	10.5 ± 0.3	94.0 (ap)	0.492 ^c	29.7 ^{d,f}	72.1	FhG-ISE (8/07)	CSG Solar (<2 μm on glass) ¹²
<i>III-V Cells</i>							
GaAs (thin film cell)	29.1 ± 0.6	0.998 (ap)	1.1272	29.78 ^g	86.7	FhG-ISE (10/18)	Alta Devices ¹³
GaAs (multicrystalline)	18.4 ± 0.5	4.011 (t)	0.994	23.2	79.7	NREL (11/95)	RTI, Ge substrate ¹⁴
InP (crystalline cell)	24.2 ± 0.5 ^h	1.008 (ap)	0.939	31.15 ^a	82.6	NREL (3/13)	NREL ¹⁵
<i>Thin Film Chalcogenide</i>							
CIGS (cell) (Cd-free)	23.35 ± 0.5	1.043 (da)	0.734	39.58 ⁱ	80.4	AIST (11/18)	Solar Frontier ¹⁶
CIGSSe (submodule)	19.6 ± 0.5	670.6 (ap)	0.688	37.63 ^j	75.8	NREL (2/21)	Avancis, 110 cells ¹⁷
CdTe (cell)	21.0 ± 0.4	1.0623 (ap)	0.8759	30.25 ^e	79.4	Newport (8/14)	First Solar, on glass ¹⁸
CZTSSe (cell)	11.3 ± 0.3	1.1761 (da)	0.5333	33.57 ^g	63.0	Newport (10/18)	DGIST, Korea ¹⁹
CZTS (cell)	10.0 ± 0.2	1.113 (da)	0.7083	21.77 ^a	65.1	NREL (3/17)	UNSW ²⁰
<i>Amorphous/Microcrystalline</i>							
Si (amorphous cell)	10.2 ± 0.3 ^{k,h}	1.001 (da)	0.896	16.36 ^e	69.8	AIST (7/14)	AIST ²¹
Si (microcrystalline cell)	11.9 ± 0.3 ^h	1.044 (da)	0.550	29.72 ^a	75.0	AIST (2/17)	AIST ²²
<i>Perovskite</i>							
Perovskite (cell)	22.6 ± 0.6 ^l	1.0189 (da)	1.178	22.73 ^j	84.4	CSIRO (10/20)	ANU ²³
Perovskite (minimodule)	21.4 ± 0.4 ^l	19.32 (da)	1.149 ^d	23.4 ^{d,b}	79.6	JET (10/21)	Microquanta, 7 cells ⁵
<i>Dye sensitized</i>							
Dye (cell)	11.9 ± 0.4 ^m	1.005 (da)	0.744	22.47 ⁿ	71.2	AIST (9/12)	Sharp ^{24,25}
Dye (minimodule)	10.7 ± 0.4 ^m	26.55 (da)	0.754 ^d	20.19 ^{d,o}	69.9	AIST (2/15)	Sharp, 7 serial cells ^{24,25}
Dye (submodule)	8.8 ± 0.3 ^m	398.8 (da)	0.697 ^d	18.42 ^{d,p}	68.7	AIST (9/12)	Sharp, 26 serial cells ^{24,25}
<i>Organic</i>							
Organic (cell)	15.2 ± 0.2 ^{h,q}	1.015 (da)	0.8467	24.24 ^c	74.3	FhG-ISE (10/20)	Fraunhofer ISE ²⁶
Organic (minimodule)	14.1 ± 0.3 ^q	19.30 (da)	0.8276 ^d	24.48 ^{d,b}	69.6	NPVIM (8/21)	ZJU/Microquanta, 7 cells ⁶
Organic (submodule)	11.7 ± 0.2 ^q	203.98 (da)	0.8177 ^d	20.68 ^{d,r}	69.3	FhG-ISE (10/19)	ZAE Bayern, 33 cells ²⁷

Note: DS = directionally solidified (including mono cast and multicrystalline), CIGS = CuIn_{1-y}Ga_ySe₂, a-Si = amorphous silicon/hydrogen alloy, nc-Si = nanocrystalline or microcrystalline silicon, CZTSSe = Cu₂ZnSnS_{4-y}Se_y, CZTS = Cu₂ZnSnS₄, (ap) = aperture area, (t) = total area, (da) = designated illumination area, FhG-ISE = Fraunhofer Institut für Solare Energiesysteme, AIST = Japanese National Institute of Advanced Industrial Science and Technology.

^aSpectral response and current-voltage curve reported in Version 50 of these tables.

^bSpectral response and current-voltage curve reported in present version of these tables.

^cSpectral response and current-voltage curve reported in Version 57 of these tables.

^dReported on a "per cell" basis.

^eSpectral responses and current-voltage curve reported in Version 45 of these tables.

^fRecalibrated from original measurement.

^gSpectral response and current-voltage curve reported in Version 53 of these tables.

^hNot measured at an external laboratory.

ⁱSpectral response and current-voltage curve reported in Version 54 of these tables.

^jSpectral response and current-voltage curve reported in Version 58 of these tables.

^kStabilized by 1000-h exposure to 1 sunlight at 50°C.

^lInitial performance. References 28 and 29 review the stability of similar devices.

^mInitial efficiency. Reference 30 reviews the stability of similar devices.

ⁿSpectral response and current-voltage curve reported in Version 41 of these tables.

^oSpectral response and current-voltage curve reported in Version 46 of these tables.

^pSpectral response and current-voltage curve reported in Version 43 of these tables.

^qInitial performance. References 31 and 32 review the stability of similar devices.

^rSpectral response and current-voltage curve reported in Version 55 of these tables.

Results are reported for cells and modules made from different semiconductors and for sub-categories within each semiconductor grouping (e.g., crystalline, polycrystalline, or directionally solidified and thin film). From Version 36 onward, spectral response information is included (when possible) in the form of a plot of the external quantum efficiency (EQE) versus wavelength, either as absolute values or normalized to the peak measured value. Current–voltage (IV) curves have also been included where possible from Version 38 onward. A graphical summary of progress over the 28 years during which the tables have been published is included in an earlier issue.³

Highest confirmed “one sun” cell and module results are reported in Tables 1–4. Any changes in the tables from those previously published¹ are set in **bold type**. In most cases, a literature reference is provided that describes either the result reported, or a similar result (readers identifying improved references are welcome to submit to the lead author). Table 1 summarizes the best-reported measurements for “one-sun” (non-concentrator) single-junction cells and submodules.

Table 2 contains what might be described as “notable exceptions” for “one-sun” single-junction cells and submodules in the above

TABLE 2 “Notable exceptions” for single-junction cells and submodules: “Top dozen” confirmed results, not class records, measured under the global AM1.5 spectrum (1000 W m^{−2}) at 25°C (IEC 60904-3: 2008 or ASTM G-173-03 global)

Classification	Efficiency (%)	Area (cm ²)	V _{oc} (V)	J _{sc} (mA/cm ²)	Fill factor (%)	Test Centre (date)	Description
<i>Cells (silicon)</i>							
Si (crystalline)	25.0 ± 0.5	4.00 (da)	0.706	42.7 ^a	82.8	Sandia (3/99)	UNSW, <i>p</i> -type PERC ³³
Si (crystalline)	25.8 ± 0.5 ^b	4.008 (da)	0.7241	42.87 ^c	83.1	FhG-ISE (7/17)	FhG-ISE, <i>n</i> -type TOPCon ³⁴
Si (crystalline)	26.0 ± 0.5 ^b	4.015 (da)	0.7323	42.05 ^d	84.3	FhG-ISE (11/19)	FhG-ISE, <i>p</i> -type TOPCon
Si (crystalline)	26.1 ± 0.3 ^b	3.9857 (da)	0.7266	42.62 ^e	84.3	ISFH (2/18)	ISFH, <i>p</i> -type rear IBC ³⁵
Si (large crystalline)	24.0 ± 0.3	244.59 (t)	0.6940	41.58 ^f	83.3	ISFH (7/19)	LONGi, <i>p</i> -type PERC ³⁶
Si (large crystalline)	25.2 ± 0.4	242.97 (ap)	0.7216	41.64 ^g	83.9	ISFH (5/21)	LONGi, <i>n</i> -type TOPCon ³⁷
Si (large crystalline)	26.6 ± 0.5	179.74 (da)	0.7403	42.5 ^h	84.7	FhG-ISE (11/16)	Kaneka, <i>n</i> -type rear IBC ¹⁰
<i>Cells (III-V)</i>							
GaInP	22.0 ± 0.3 ^b	0.2502 (ap)	1.4695	16.63 ⁱ	90.2	NREL (1/19)	NREL, rear HJ, strained AlInP ³⁸
<i>Cells (chalcogenide)</i>							
CdTe (thin-film)	22.1 ± 0.5	0.4798 (da)	0.8872	31.69 ^j	78.5	Newport (11/15)	First Solar on glass ³⁹
CZTSSe (thin-film)	13.0 ± 0.1	0.1072 (ap)	0.5294	33.58^k	72.9	NREL (x/21)	NJUPT (10% Ag)⁴⁰
CZTS (thin-film)	11.0 ± 0.2	0.2339 (da)	0.7306	21.74 ^f	69.3	NREL (3/17)	UNSW on glass ⁴¹
<i>Cells (other)</i>							
Perovskite (thin-film)	25.5 ± 0.8 ^{l,m}	0.0954 (ap)	1.1885	25.74 ^f	83.2	Newport (7/20)	UNIST Ulsan ⁴²
Organic (thin-film)	18.2 ± 0.2 ⁿ	0.0322 (da)	0.8965	25.72 ^f	78.9	NREL (10/20)	SJTU Shanghai/Beihang U.
Dye sensitized	12.25 ± 0.4 ^o	0.0963 (ap)	1.0203	15.17 ^d	79.1	Newport (8/19)	EPFL ⁴³

Note: DS = directionally solidified (including mono cast and multicrystalline), CIGS_{Se} = CuInGaS_{Se}, CZTSSe = Cu₂ZnSnS_{4-y}Se_y, CZTS = Cu₂ZnSnS₄, (ap) = aperture area, (t) = total area, (da) = designated illumination area, AIST, Japanese National Institute of Advanced Industrial Science and Technology, NREL, National Renewable Energy Laboratory, FhG-ISE, Fraunhofer-Institut für Solare Energiesysteme, ISFH, Institute for Solar Energy Research, Hamelin.

^aSpectral response reported in Version 36 of these tables.

^bNot measured at an external laboratory.

^cSpectral response and current–voltage curves reported in Version 51 of these tables.

^dSpectral response and current–voltage curves reported in Version 55 of these tables.

^eSpectral response and current–voltage curve reported in Version 52 of these tables.

^fSpectral response and current–voltage curves reported in Version 57 of these tables.

^gSpectral response and current–voltage curve reported in Version 58 of these tables.

^hSpectral response and current–voltage curves reported in Version 50 of these tables.

ⁱSpectral response and current–voltage curve reported in Version 54 of these tables.

^jSpectral response and/or current–voltage curves reported in Version 46 of these tables.

^kSpectral response and current–voltage curves reported in the present version of these tables.

^lStability not investigated. References 25 and 26 document stability of similar devices.

^mMeasured using 10-point IV sweep with constant voltage bias until current change rate <0.07%/min.

ⁿLong term stability not investigated. References 28 and 29 document stability of similar devices.

^oLong term stability not investigated. Reference 30 documents stability of similar devices.

TABLE 3 Confirmed multiple-junction terrestrial cell and submodule efficiencies measured under the global AM1.5 spectrum (1000 W/m²) at 25°C (IEC 60904-3: 2008 or ASTM G-173-03 global)

Classification	Efficiency (%)	Area (cm ²)	Voc (V)	Jsc (mA/cm ²)	Fill factor (%)	Test center (date)	Description
<i>III-V Multijunctions</i>							
5 junction cell (bonded) (2.17/1.68/1.40/1.06/.73 eV)	38.8 ± 1.2	1.021 (ap)	4.767	9.564	85.2	NREL (7/13)	Spectrolab, 2-terminal ⁴⁴
InGaP/GaAs/InGaAs	37.9 ± 1.2	1.047 (ap)	3.065	14.27 ^a	86.7	AIST (2/13)	Sharp, 2 term. ⁴⁵
GaInP/GaAs (monolithic)	32.8 ± 1.4	1.000 (ap)	2.568	14.56 ^b	87.7	NREL (9/17)	LG Electronics, 2 term.
<i>Multijunctions with c-Si</i>							
GaInP/GaInAsP/Si (wafer bonded)	35.9 ± 1.3 ^c	3.987 (ap)	3.248	13.11 ^d	84.3	FhG-ISE (4/20)	Fraunhofer ISE, 2-term. ⁴⁶
GaInP/GaAs/Si (mech. stack)	35.9 ± 0.5 ^b	1.002 (da)	2.52/0.681	13.6/11.0	87.5/78.5	NREL (2/17)	NREL/CSEM/EPFL, 4-term. ⁴⁵
GaInP/GaAs/Si (monolithic)	25.9 ± 0.9 ^c	3.987 (ap)	2.647	12.21 ^e	80.2	FhG-ISE (6/20)	Fraunhofer ISE, 2-term. ⁴⁷
GaAsP/Si (monolithic)	23.4 ± 0.3	1.026 (ap)	1.732	17.34 ^f	77.7	NREL (5/20)	OSU/UNSW/SolAero, 2-term ⁴⁸
GaAs/Si (mech. stack)	32.8 ± 0.5 ^c	1.003 (da)	1.09/0.683	28.9/11.1 ^g	85.0/79.2	NREL (12/16)	NREL/CSEM/EPFL, 4-term. ⁴⁹
Perovskite/Si (2-terminal)	29.5 ± 0.5 ^h	1.121 (da)	1.884	20.26 ^d	77.3	NREL (12/20)	Oxford PV
GaInP/GaInAs/Ge; Si (spectral split minimodule)	34.5 ± 2.0	27.83 (ap)	2.66/0.65	13.1/9.3	85.6/79.0	NREL (4/16)	UNSW/Azur/Trina, 4-term. ⁵⁰
<i>Other Multijunctions</i>							
Perovskite/CIGS	24.2 ± 0.7 ^h	1.045 (da)	1.768	19.24 ^f	72.9	FhG-ISE (1/20)	HZB, 2-terminal ⁵¹
Perovskite/perovskite	24.2 ± 0.8 ^h	1.041(da)	1.986	15.93 ^f	76.6	JET (12/19)	Nanjing U, 2-term. ⁵²
Perovskite/perovskite (minimodule)	21.7 ± 0.6^h	20.25(da)	2.009	14.22	75.9	JET (8/21)	Nanjing U, 2-term.⁵²
a-Si/nc-Si/nc-Si (thin-film)	14.0 ± 0.4 ^{i,c}	1.045 (da)	1.922	9.94 ^j	73.4	AIST (5/16)	AIST, 2-term. ⁵³
a-Si/nc-Si (thin-film cell)	12.7 ± 0.4 ^{i,c}	1.000(da)	1.342	13.45 ^k	70.2	AIST (10/14)	AIST, 2-term. ⁵⁴
<i>"Notable Exceptions"</i>							
GaInP/GaAs (mqw)	32.9 ± 0.5 ^c	0.250 (ap)	2.500	15.36 ^l	85.7	NREL (1/20)	NREL/UNSW, multiple QW
GaInP/GaAs/GaInAs	37.8 ± 1.4	0.998 (ap)	3.013	14.60 ^l	85.8	NREL (1/18)	Microlink (ELO) ⁵⁵
GaInP/GaAs (mqw)/GaInAs	39.5 ± 0.5^c	0.242 (ap)	2.997	15.44^m	85.3	NREL (9/21)	NREL, multiple QW
6 junction (monolithic) (2.19/1.76/1.45/1.19/.97/ .7 eV)	39.2 ± 3.2 ^c	0.247 (ap)	5.549	8.457 ⁿ	83.5	NREL (11/18)	NREL, inv. metamorphic ⁵⁶
Perovskite/perovskite	26.4 ± 0.8 ^h	0.0494(da)	2.048	16.54 ^d	77.9	JET (2/21)	Nanjing U, 2-term. ⁵²
GaInP/AlGaAs/CIGS	28.1 ± 1.2 ^c	0.1386(da)	2.952	11.72 ^d	81.1	AIST (1/21)	AIST/FhG-ISE, 2-term. ⁵⁷

Note: a-Si = amorphous silicon/hydrogen alloy, nc-Si = nanocrystalline or microcrystalline silicon, (ap) = aperture area, (t) = total area, (da) = designated illumination area, FhG-ISE = Fraunhofer Institut für Solare Energiesysteme, AIST = Japanese National Institute of Advanced Industrial Science and Technology.

^aSpectral response and current-voltage curve reported in Version 42 of these tables.

^bSpectral response and current-voltage curve reported in the Version 51 of these tables.

^cNot measured at an external laboratory.

^dSpectral response and current-voltage curve reported in Version 58 of these tables.

^eSpectral response and current-voltage curve reported in Version 57 of these tables.

^fSpectral response and current-voltage curve reported in Version 56 of these tables.

^gSpectral response and current-voltage curve reported in Version 52 of these tables.

^hInitial efficiency. References 36 and 37 review the stability of similar perovskite-based devices.

ⁱStabilized by 1000-h exposure to 1 sun light at 50°C.

^jSpectral response and current-voltage curve reported in Version 49 of these tables.

^kSpectral responses and current-voltage curve reported in Version 45 of these tables.

^lSpectral response and current-voltage curve reported in Version 53 of these tables.

^mSpectral response and current-voltage curves reported in the present version of these tables.

ⁿSpectral response and current-voltage curve reported in Version 54 of these tables.

TABLE 4 Confirmed non-concentrating terrestrial module efficiencies measured under the global AM1.5 spectrum (1000 W/m²) at a cell temperature of 25°C (IEC 60904-3: 2008 or ASTM G-173-03 global)

Classification	Effic. (%)	Area (cm ²)	V _{oc} (V)	I _{sc} (A)	FF (%)	Test center (date)	Description
Si (crystalline)	24.4 ± 0.5	13,177 (da)	79.5	5.04 ^a	80.1	AIST (9/16)	Kaneka (108 cells) ¹⁰
Si (multicrystalline)	20.4 ± 0.3	14,818 (ap)	39.90	9.833 ^b	77.2	FhG-ISE (10/19)	Hanwha Q Cells (60 cells) ⁵⁸
GaAs (thin-film)	25.1 ± 0.8	866.45 (ap)	11.08	2.303 ^c	85.3	FhG-ISE (11/17)	Alta Devices ⁵⁹
CIGS (Cd-free)	19.2 ± 0.5	841 (ap)	48.0	0.456 ^c	73.7	AIST (1/17)	Solar Frontier (70 cells) ⁶⁰
CdTe (thin-film)	19.0 ± 0.9	23,573 (da)	227.8	2.560 ^b	76.6	FhG-ISE (9/19)	First Solar ⁶¹
a-Si/nc-Si (tandem)	12.3 ± 0.3 ^d	14,322 (t)	280.1	0.902 ^e	69.9	ESTI (9/14)	TEL Solar, Trubbach Labs ⁶²
Perovskite	17.9 ± 0.5 ^f	804 (da)	58.7	0.323 ^g	76.1	AIST (1/20)	Panasonic (55 cells) ⁶³
Organic	8.7 ± 0.3 ^h	802 (da)	17.47	0.569 ⁱ	70.4	AIST (5/14)	Toshiba ⁶⁴
Multijunction							
InGaP/GaAs/InGaAs	31.2 ± 1.2	968 (da)	23.95	1.506	83.6	AIST (2/16)	Sharp (32 cells) ⁶⁵
“Notable Exception”							
CIGS (large)	18.6 ± 0.6	10,858 (ap)	58.00	4.545 ^b	76.8	FhG-ISE (10/19)	Miasole ⁶⁶

Note: CIGSS = CuInGaSSe, a-Si = amorphous silicon/hydrogen alloy, a-SiGe = amorphous silicon/germanium/hydrogen alloy, nc-Si = nanocrystalline or microcrystalline silicon, Effic. = efficiency, (t) = total area, (ap) = aperture area, (da) = designated illumination area, FF = fill factor.

^aSpectral response and current voltage curve reported in Version 49 of these tables.

^bSpectral response and current-voltage curve reported in Version 55 of these tables.

^cSpectral response and current-voltage curve reported in Version 50 or 51 of these tables.

^dStabilised at the manufacturer to the 2% level following IEC procedure of repeated measurements.

^eSpectral response and/or current-voltage curve reported in Version 46 of these tables.

^fInitial performance. References 25 and 26 review the stability of similar devices.

^gSpectral response and current-voltage curve reported in Version 57 of these tables.

^hInitial performance. References 28 and 29 review the stability of similar devices.

ⁱSpectral response and current-voltage curve reported in Version 45 of these tables.

category. While not conforming to the requirements to be recognized as a class record, the devices in Table 2 have notable characteristics that will be of interest to sections of the photovoltaic community, with entries based on their significance and timeliness. To encourage discrimination, the table is limited to nominally 12 entries with the present authors having voted for their preferences for inclusion. Readers who have suggestions of notable exceptions for inclusion into this or subsequent tables are welcome to contact any of the authors with full details. Suggestions conforming to the guidelines will be included on the voting list for a future issue.

Table 3 was first introduced in Version 49 of these tables and summarizes the growing number of cell and submodule results involving high efficiency, one-sun multiple-junction devices (previously reported in Table 1). Table 4 shows the best results for one-sun modules, both single- and multiple-junction, while Table 5 shows the best results for concentrator cells and concentrator modules. A small number of “notable exceptions” are also included in Tables 3 to 5.

2 | NEW RESULTS

Six new results are reported in the present version of these tables. The first new result in Table 1 (“one-sun cells and submodules”) is 26.3% total area efficiency for a large area silicon heterojunction (HJT) cell fabricated on an M6 wafer (274 cm²) by LONGi Solar⁴ and measured by the Institute für Solarenergieforschung (ISFH). This was

a bifacial cell measured on a reflective gold-plated brass chuck with frontside busbar and rearside grid resistance neglecting contacting. The result is a large improvement over the 25.3% HJT result also from LONGi on an M2 wafer (245 cm²) reported in the previous version of these tables (also total area, but misreported there as aperture area; also Sanyo, not Sharp, pioneered the development of HJT cells).¹ Soon afterwards, Suzhou Maxwell Technologies Co. Ltd in conjunction with Anhui Huasun Energy Co. Ltd achieved the same 25.3% efficiency for a HJT cell on a larger M6 wafer, followed by Sundrive Solar Pty Ltd in conjunction with Suzhou Maxwell Technologies Co. Ltd achieving 25.8% HJT cell efficiency also on an M6 wafer, the latter using Cu plated contacts. Since the new 26.3% result is clearly the highest confirmed total area Si cell efficiency yet reported, it has provided the opportunity to introduce a new category into Table 1, the highest total area Si cell result.

The two other new results in Table 1 are for minimodules, defined for these tables as a package of interconnected cells of area <200 cm². The first is 21.4% efficiency for a 19.3-cm² perovskite cell minimodule fabricated by Hangzhou Microquanta Semiconductor Co. Ltd (Microquanta)⁵ and measured at the Japan Electrical Safety and Environment Technology Laboratories (JET). The second is 14.1% efficiency for another 19.3-cm² minimodule but using organic solar cells fabricated by Zhejiang University (ZJU)⁶ in conjunction with Microquanta and measured by the Chinese National Photovoltaic Industry Metrology and Testing Center (NPVM). Along with other emerging technologies, perovskite and organic cells and modules may

TABLE 5 Terrestrial concentrator cell and module efficiencies measured under the ASTM G-173-03 direct beam AM1.5 spectrum at a cell temperature of 25°C (except where noted for the hybrid and luminescent modules)

Classification	Effic. (%)	Area (cm ²)	Intensity ^a (suns)	Test center (date)	Description
<u>Single Cells</u>					
GaAs	30.5 ± 1.0 ^b	0.10043 (da)	258	NREL (10/18)	NREL, 1 junction (1 J)
Si	27.6 ± 1.2 ^c	1.00 (da)	92	FhG-ISE (11/04)	Amonix back-contact ⁶⁷
CIGS (thin-film)	23.3 ± 1.2 ^{d,e}	0.09902 (ap)	15	NREL (3/14)	NREL ⁶⁸
<u>Multijunction cells</u>					
AlGaInP/AlGaAs/GaAs/GaInAs(3) (2.15/1.72/1.41/1.17/0.96/0.70 eV)	47.1 ± 2.6 ^{d,f}	0.099 (da)	143	NREL (3/19)	NREL, 6 J inv. metamorphic ⁵⁶
GaInP/GaAs; GaInAsP/GaInAs	46.0 ± 2.2 ^g	0.0520 (da)	508	AIST (10/14)	Soitec/CEA/FhG-ISE 4 J bonded ⁶⁹
GaInP/GaAs/GaInAs/GaInAs	45.7 ± 2.3 ^{d,h}	0.09709 (da)	234	NREL (9/14)	NREL, 4 J monolithic ⁷⁰
InGaP/GaAs/InGaAs	44.4 ± 2.6 ⁱ	0.1652 (da)	302	FhG-ISE (4/13)	Sharp, 3 J inverted metamorphic ⁷¹
GaInAsP/GaInAs	35.5 ± 1.2 ^{d,j}	0.10031 (da)	38	NREL (10/17)	NREL 2-junction (2 J) ⁷²
<u>Minimodule</u>					
GaInP/GaAs; GaInAsP/GaInAs	43.4 ± 2.4 ^{d,k}	18.2 (ap)	340 ^l	FhG-ISE (7/15)	Fraunhofer ISE 4 J (lens/cell) ⁷³
<u>Submodule</u>					
GaInP/GaInAs/Ge; Si	40.6 ± 2.0 ^k	287 (ap)	365	NREL (4/16)	UNSW 4 J split spectrum ⁷⁴
<u>Modules</u>					
Si	20.5 ± 0.8 ^d	1875 (ap)	79	Sandia (4/89) ^l	Sandia/UNSW/ENTECH (12 cells) ⁷⁵
Three Junction (3 J)	35.9 ± 1.8 ^m	1,092 (ap)	N/A	NREL (8/13)	Amonix ⁷⁶
Four Junction (4 J)	38.9 ± 2.5 ⁿ	812.3 (ap)	333	FhG-ISE (4/15)	Soitec ⁷⁷
<u>Hybrid Module^o</u>					
4-Junction (4 J)/bifacial c-Si	34.2 ± 1.9 ^{d,o}	1,088 (ap)	CPV/PV	FhG-ISE (9/19)	FhG-ISE (48/8 cells; 4 T) ⁷⁸
<u>“Notable Exceptions”</u>					
Si (large area)	21.7 ± 0.7	20.0 (da)	11	Sandia (9/90) ^l	UNSW laser grooved ⁷⁹
Luminescent Minimodule ^o	7.1 ± 0.2	25 (ap)	2.5 ^p	ESTI (9/08)	ECN Petten, GaAs cells ⁸⁰
4 J Minimodule	41.4 ± 2.6 ^d	121.8 (ap)	230	FhG-ISE (9/18)	FhG-ISE, 10 cells ⁷³

Note: Following the normal convention, efficiencies calculated under this direct beam spectrum neglect the diffuse sunlight component that would accompany this direct spectrum. These direct beam efficiencies need to be multiplied by a factor estimated as 0.8746 to convert to thermodynamic efficiencies.⁸¹

CIGS = CuInGaSe₂, Effic. = efficiency, (da) = designated illumination area, (ap) = aperture area, NREL = National Renewable Energy Laboratory, FhG-ISE = Fraunhofer-Institut für Solare Energiesysteme. 4-terminal module with external dual-axis tracking. Power rating of CPV follows IEC 62670–3 standard, front power rating of flat plate PV based on IEC 60904-3, -5, -7, -10, and 60891 with modified current translation approach; rear power rating of flat plate PV based on IEC TS 60904-1-2 and 60891.

^aOne sun corresponds to direct irradiance of 1000 W m⁻².

^bSpectral response and current–voltage curve reported in Version 53 of these tables.

^cMeasured under a low aerosol optical depth spectrum similar to ASTM G-173-03 direct.⁸²

^dNot measured at an external laboratory.

^eSpectral response and current–voltage curve reported in Version 44 of these tables.

^fSpectral response and current–voltage curve reported in Version 54 of these tables.

^gSpectral response and current–voltage curve reported in Version 45 of these tables.

^hSpectral response and current–voltage curve reported in Version 46 of these tables.

ⁱSpectral response and current–voltage curve reported in Version 42 of these tables.

^jSpectral response and current–voltage curve reported in Version 51 of these tables.

^kDetermined at IEC 62670–1 CSTC reference conditions.

^lRecalibrated from original measurement.

^mReferenced to 1,000 W/m² direct irradiance and 25°C cell temperature using the prevailing solar spectrum and an in-house procedure for temperature translation.

ⁿMeasured under IEC 62670-1 reference conditions following the current IEC power rating draft 62670-3.

^oThermodynamic efficiency. Hybrid and luminescent modules measured under the ASTM G-173-03 or IEC 60904-3: 2008 global AM1.5 spectrum at a cell temperature of 25°C.

^pGeometric concentration.

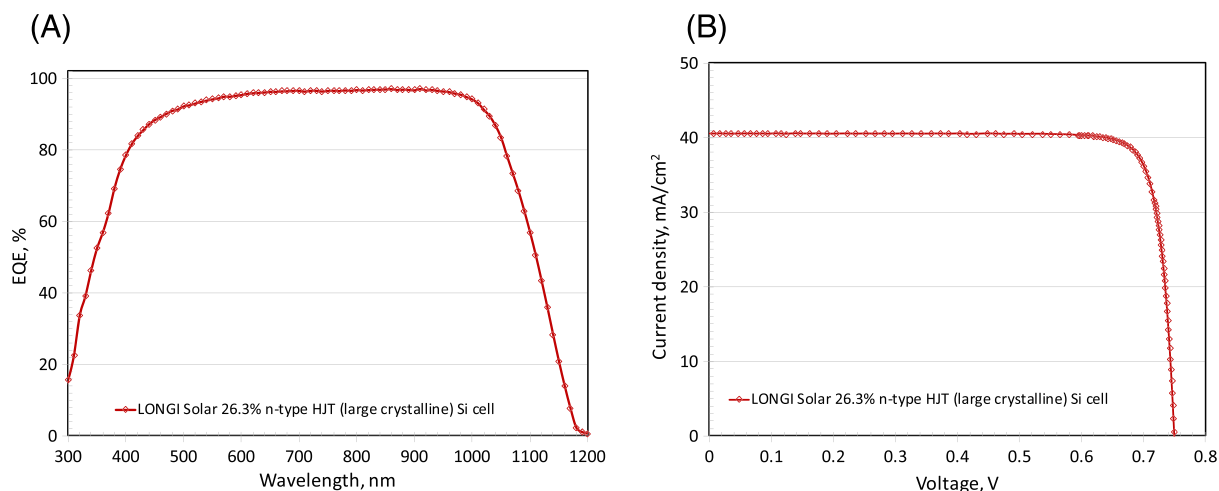


FIGURE 1 (A) External quantum efficiency (EQE) for the new Si cell result reported in this issue; (B) corresponding current density–voltage (JV) curve

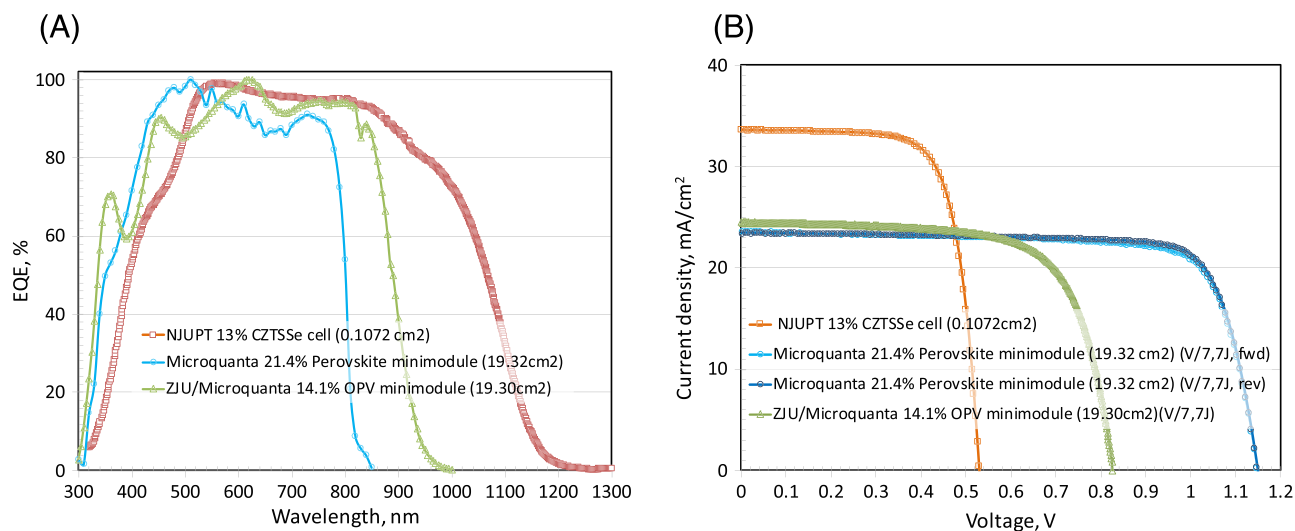


FIGURE 2 (A) External quantum efficiency (EQE) for the new CZTSSe cell and perovskite and organic cell minimodules reported in this issue (results are normalized); (B) corresponding current density–voltage (JV) curves

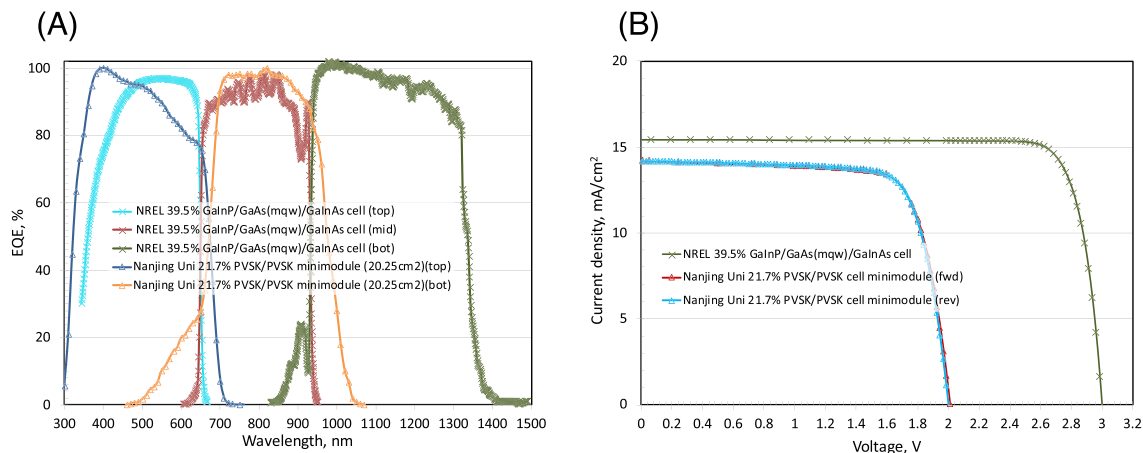


FIGURE 3 (A) External quantum efficiency (EQE) for the new multijunction cell and minimodule results reported in this issue (results are normalized); (B) corresponding current density–voltage (JV) curves (PVSK: perovskite)

not demonstrate the same level of stability as more established cell technologies, with references to this aspect given in the footnotes to Table 1.

There is one new result in Table 2 (one-sun “notable exceptions”). An efficiency of 13.0% is reported for a small-area 0.1-cm² CZTSSe [(Cu,Ag)₂ZnSn(S,Se)₄] cell fabricated by the Nanjing University of Posts and Telecommunications (NJUPT) and measured by the US National Renewable Energy Laboratory (NREL). The cell absorber material was alloyed with 10% Ag. Cell area is too small for classification as an outright record, with solar cell efficiency targets in governmental research programs generally specified in terms of a cell area of 1 cm² or larger.^{7–9}

There are two new results reported in Table 3 relating to one-sun, multijunction devices. The first is 21.7% efficiency for a 20-cm² perovskite/perovskite tandem minimodule fabricated by Nanjing University and measured by the Japan Electrical Safety & Environment Technology Laboratories (JET). The second “notable exception” result is for a two-terminal, triple junction Group III-V tandem device where an efficiency of 39.5% is reported for a small area 0.242-cm² GaInP/GaAs (mqw)/GaInAs cell fabricated and measured by NREL, where “mqw” indicates multiple quantum wells were incorporated into the GaAs layer. This is the highest efficiency we have ever reported for a one-sun cell although cell area is again too small for classification as an outright record.

The EQE spectra for the new silicon cell reported in the present issue of these tables are shown in Figure 1A, with Figure 1B showing the current density–voltage (JV) curve for the same device. Figure 2A, B show the corresponding EQE and JV curves for the new CZTSSe cell plus organic and perovskite minimodule results, while Figure 3A,B show these for the new multijunction cell and minimodule results.

3 | DISCLAIMER

While the information provided in the tables is provided in good faith, the authors, editors and publishers cannot accept direct responsibility for any errors or omissions.

ACKNOWLEDGEMENTS

The Australian Centre for Advanced Photovoltaics commenced operation in February 2013 with support from the Australian Government through the Australian Renewable Energy Agency (ARENA). The Australian Government does not accept responsibility for the views, information or advice expressed herein. The work at NREL was supported by the U.S. Department of Energy under Contract No. DE-AC36-08-GO28308 with the National Renewable Energy Laboratory. The work at AIST was supported in part by the Japanese New Energy and Industrial Technology Development Organisation (NEDO) under the Ministry of Economy, Trade and Industry (METI).

DATA AVAILABILITY STATEMENT

The data that support the findings of this study are available from the corresponding author upon reasonable request.

ORCID

Martin A. Green  <https://orcid.org/0000-0002-8860-396X>

REFERENCES

- Green MA, Dunlop ED, Hohl-Ebinger J, Yoshita M, Kopidakis N, Hao XJ. Solar cell efficiency tables (Version 58). *Prog Photovolt: Res Appl*. 2021;29(7):657–667.
- Green MA, Emery K, Hishikawa Y, Warta W. Solar cell efficiency tables (Version 33). *Prog Photovolt: Res Appl*. 2009;17(1):85–94.
- Green MA, Dunlop ED, Hohl-Ebinger J, Yoshita M, Kopidakis N, Hao XJ. Solar cell efficiency tables (Version 57). *Prog Photovolt: Res Appl*. 2021;29(1):3–15.
- LONGi breaks three more world records for solar cell efficiency. Press Release, 2 June 2021. https://en.longi-solar.com/home/events/press_detail/id/335.html
- <http://www.microquanta.com/en/>
- Wang D, Zhou G, Li Y, et al. High-Performance Organic Solar Cells from Non-Halogenated Solvents. *Adv Funct Mater*. 2021;2107827. <https://doi.org/10.1002/adfm.202107827>
- Program milestones and decision points for single junction thin films. Annual Progress Report 1984, Photovoltaics, Solar Energy Research Institute, Report DOE/CE-0128, June 1985, 7.
- Sakata I, Tanaka Y, Koizawa K. Japan's New National R&D Program for Photovoltaics. Photovoltaic Energy Conversion, Conference Record of the 2006 IEEE 4th World Conference, May 2008; 1: 1–4.
- Jäger-Waldau, A (Ed.). PVNET: European Roadmap for PV R&D, EUR 21087 EN, 2004.
- Yoshikawa K, Kawasaki H, Yoshida W, et al. Silicon heterojunction solar cell with interdigitated back contacts for a photoconversion efficiency over 26%. *Nat Energy*. 2017;2(5):17032.
- Moslehi MM, Kapur P, Kramer J, Rana V, Seutter S, Deshpande A, Stalcup T, Kommera S, Ashjaee J, Calcaterra A, Grupp D, Dutton D, Brown R. World-record 20.6% efficiency 156 mm x 156 mm full-square solar cells using low-cost kerfless ultrathin epitaxial silicon & porous silicon lift-off technology for industry-leading high-performance smart PV modules. PV Asia Pacific Conference (APVI A/PVAP), 24 October 2012.
- Keevers MJ, Young TL, Schubert U, Green MA. 10% efficient CSG minimodules. 22nd European Photovoltaic Solar Energy Conference, Milan, September 2007.
- Kayes BM, Nie H, Twist R, Spruytte SG, Reinhardt F, Kizilyalli IC, Higashi GS. 27.6% conversion efficiency, a new record for single-junction solar cells under 1 sun illumination. Proceedings of the 37th IEEE Photovoltaic Specialists Conference, 2011.
- Venkatasubramanian R, O'Quinn BC, Hills JS, Sharps PR, Timmons ML, Hutchby JA, Field H, Ahrenkiel A, Keyes B. 18.2% (AM1.5) efficient GaAs solar cell on optical-grade polycrystalline Ge substrate. Conference Record, 25th IEEE Photovoltaic Specialists Conference, Washington, 1997; 31–36.
- Wanlass M. Systems and methods for advanced ultra-high-performance InP solar cells. US Patent 9,590,131 B2, 7 March 2017.
- Nakamura M, Yamaguchi K, Kimoto Y, Yasaki Y, Kato T, Sugimoto H. Cd-free Cu (In,Ga)(Se,S)₂ thin-film solar cell with a new world record efficacy of 23.35%, 46th IEEE PVSC, Chicago, IL, June 19, 2019, (see also http://www.solar-frontier.com/eng/news/2019/0117_press.html)
- Diermann R. Avancis claims 19.64% efficiency for CIGS module, PV Magazine International, March 4, 2021. (<https://www.pv-magazine.com/2021/03/04/avancis-claims-19-64-efficiency-for-cigs-module/>)
- First Solar Press Release, First solar builds the highest efficiency thin film PV cell on record, 5 August 2014.
- https://en.dgist.ac.kr/site/dgist_eng/menu/984.do (accessed 28 October 2018).

20. Yan C, Huang J, Sun K, et al. $\text{Cu}_2\text{ZnSnS}_4$ solar cells with over 10% power conversion efficiency enabled by heterojunction heat treatment. *Nat Energy*. 2018;3(9):764-772.
21. Matsui T, Bidiville A, Sai H, et al. High-efficiency amorphous silicon solar cells: impact of deposition rate on metastability. *Appl Phys Lett*. 2015;106(5):053901. <https://doi.org/10.1063/1.4907001>
22. Sai H, Matsui T, Kumagai H, Matsubara K. Thin-film microcrystalline silicon solar cells: 11.9% efficiency and beyond. *Appl Phys Exp*. 2018;11(2):022301.
23. Peng J, Walter D, Ren Y, et al. Nanoscale localized contacts for high fill factors in polymer-passivated perovskite solar cells. *Science*. 2021;371(6527):390-395.
24. Han L, Fukui A, Chiba Y, et al. Integrated dye-sensitized solar cell module with conversion efficiency of 8.2%. *Appl Phys Lett*. 2009;94:013305. <https://doi.org/10.1063/1.3054160>
25. Komiya R, Fukui A, Murofushi N, Koide N, Yamanaka R, Katayama H. Improvement of the conversion efficiency of a monolithic type dye-sensitized solar cell module. Technical Digest, 21st International Photovoltaic Science and Engineering Conference, Fukuoka, November 2011; 2C-50-08.
26. Würfel U, Herterich J, List M, et al. A 1 cm^2 organic solar cell with 15.2% certified efficiency: detailed characterization and identification of optimization potential. *Sol. RRL*. 2021;5(4):2000802. <https://doi.org/10.1002/solr.202000802>
27. https://www.encl.de/fileadmin/user_upload/PR_opv-record_.pdf (accessed 11 November, 2019).
28. Han Y, Meyer S, Dkhissi Y, et al. Degradation observations of encapsulated planar $\text{CH}_3\text{NH}_3\text{PbI}_3$ perovskite solar cells at high temperatures and humidity. *J Mater Chem A*. 2015;3(15):8139-8147.
29. Yang Y, You J. Make perovskite solar cells stable. *Nature*. 2017;544(7649):155-156.
30. Krašovec UO, Bokalić M, Topić M. Ageing of DSSC studied by electroluminescence and transmission imaging. *Solar Energy Mater Solar Cells*. 2013;117:67-72.
31. Tanenbaum DM, Hermenau M, Voroshazi E, et al. The ISOS-3 interlaboratory collaboration focused on the stability of a variety of organic photovoltaic devices. *RSC Adv*. 2012;2(3):882-893.
32. (a) Krebs FC (Ed). *Stability and Degradation of Organic and Polymer Solar Cells*. Chichester: Wiley; 2012; (b) Jorgensen M, Norrman K, Gevorgyan SA, Tromholt T, Andreasen B, Krebs FC. Stability of polymer solar cells. *Adv Mater* 2012; 24: 580-612, 5.
33. Green MA. The Passivated Emitter and Rear Cell (PERC): From conception to mass production. *Solar Energy Mater Solar Cells*. 2015;143:190-197.
34. Richter A, Benick J, Feldmann F, Fell A, Hermle M, Glunz SW. n-Type Si solar cells with passivating electron contact: Identifying sources for efficiency limitations by wafer thickness and resistivity variation. *Solar Energy Mater Solar Cells*. 2017;173:96-105.
35. Haase F, Klamt C, Schäfer S, et al. Laser contact openings for local poly-Si-metal contacts enabling 26.1%-efficient POLO-IBC solar cells. *Solar Energy Mater Solar Cells*. 2018;186:184-193.
36. Wang Q. Status of crystalline silicon PERC solar cells. NIST/UL Workshop on Photovoltaic Materials Durability, Gaithersburg, MD USA, Dec 12-13, 2019; 1, 15.
37. https://en.longi-solar.com/home/events/press_detail/id/331.html
38. NREL, private communication, 22 May 2019.
39. First Solar Press Release. First Solar Achieves yet another cell conversion efficiency world record, 24 February 2016.
40. <https://www.njupt.edu.cn/en/2021/0525/c13237a194534/page.psp>
41. Sun K, Yan C, Liu F, et al. Beyond 9% efficient kesterite $\text{Cu}_2\text{ZnSnS}_4$ solar cell: fabricated by using $\text{Zn}_{1-x}\text{Cd}_x\text{S}$ buffer layer. *Adv Energy Mater*. 2016;6(12):1600046. <https://doi.org/10.1002/aenm.201600046>
42. Jeong M, Choi IW, Go EM, et al. Stable perovskite solar cells with efficiency exceeding 24.8% and 0.3-V voltage loss. *Science*. 2020;369(6511):1615-1620. <https://doi.org/10.1126/science.abb7167>
43. <https://www.epfl.ch/labs/lspm/>; <https://www.epfl.ch/labs/lpi/> (accessed 28 October 2019).
44. Sasaki K, Agui T, Nakaido K, Takahashi N, Onitsuka R, Takamoto T. Proceedings, 9th International Conference on Concentrating Photovoltaics Systems, Miyazaki, Japan 2013.
45. Essig S, Allebé C, Remo T, et al. Raising the one-sun conversion efficiency of III-V/Si solar cells to 32.8% for two junctions and 35.9% for three junctions. *Nat Energy*. 2017;2(9):17144. <https://doi.org/10.1038/nenergy.2017.144>
46. Müller R, Schygulla P, Lackner D, Höhn O, Hauser H, Richter A, Fell A, Bläsi B, Predan F, Benick J, Hermle M, Dimroth F, Glunz SW. Silicon-based monolithic triple-junction solar cells with conversion efficiency >34%. 37th European Photovoltaic Solar Energy Conference and Exhibition, 574-578, DOI: <https://doi.org/10.4229/EUPVSEC20202020-3AO.7.2>
47. Feifel M, Lackner D, Schön J, et al. Epitaxial GaInP/GaAs/Si triple-junction solar cell with 25.9% AM1.5g efficiency enabled by transparent metamorphic $\text{Al}_x\text{Ga}_{1-x}\text{As}_y\text{P}_{1-y}$ step-graded buffer structures. *Sol. RRL*. 2021;5:2000763. <https://doi.org/10.1002/solr.202000763>
48. Grassman TJ, Chmielewski DJ, Carnevale SD, Carlin JA, Ringel SA. $\text{GaAs}_{0.75}\text{P}_{0.25}/\text{Si}$ dual-junction solar cells grown by MBE and MOCVD. *IEEE J Photovolt*. 2016;6(1):326-331.
49. <https://www.oxfordpv.com/news/oxford-pv-hits-new-world-record-solar-cell>
50. Green MA, Keevers MJ, Concha Ramon B, Jiang Y, Thomas I, Lasich JB, Verlinden PJ, Yang Y, Zhang X, Emery K, Moriarty T, King RR, Bensch W. Improvements in sunlight to electricity conversion efficiency: above 40% for direct sunlight and over 30% for global. Paper 1AP.1.2, European Photovoltaic Solar Energy Conference 2015, Hamburg, September 2015.
51. <https://www.pv-magazine.com/2019/09/11/hzb-hits-23-26-efficiency-with-cigs-perovskite-tandem-cell/> (accessed 28 October 2019).
52. Lin R, Xiao K, Qin ZY, et al. Monolithic all-perovskite tandem solar cells with 24.8% efficiency exploiting comproportionation to suppress Sn (ii) oxidation in precursor ink. *Nat Energy*. 2019;4(10):864-873.
53. Sai H, Matsui T, Koida T, Matsubara K. Stabilized 14.0%-efficient triple-junction thin-film silicon solar cell. *Appl Phys Lett*. 2016;109(18):183506. <https://doi.org/10.1063/1.49669986>
54. Matsui T, Maejima K, Bidiville A, et al. High-efficiency thin-film silicon solar cells realized by integrating stable a-Si:H absorbers into improved device design. *Jpn J Appl Phys*. 2015;54:08KB10. <https://doi.org/10.7567/JJAP.54.08KB10>
55. <http://mldevices.com/index.php/news/> (accessed 28 October 2018).
56. Geisz JF, Steiner MA, Jain N, et al. Building a six-junction inverted metamorphic concentrator solar cell. *IEEE J Photovolt*. 2018;8(2):626-632.
57. Makita K, Kamikawa Y, Mizuno H, et al. III-V// $\text{Cu}_x\text{In}_{1-y}\text{Ga}_y\text{Se}_2$ multi-junction solar cells with 27.2% efficiency fabricated using modified smart stack technology with Pd nanoparticle array and adhesive material. *Prog Photovolt Res Appl*. 2021;29:887-898. <https://doi.org/10.1002/pip.3398>
58. <https://www.hanwha-qcells.com> (accessed 28 October 2019).
59. Mattos LS, Scully SR, Syfu M, Olson E, Yang L, Ling C, Kayes BM, He G. New module efficiency record: 23.5% under 1-sun illumination using thin-film single-junction GaAs solar cells. Proceedings of the 38th IEEE Photovoltaic Specialists Conference, 2012.
60. Sugimoto H. High efficiency and large volume production of CIS-based modules. 40th IEEE Photovoltaic Specialists Conference, Denver, June 2014.

61. <http://www.firstsolar.com/en-AU/-/media/First-Solar/Technical-Documents/Series-6-Datasheets/Series-6-Datasheet.ashx> (accessed 28 October 2019).
62. Cashmore JS, Apolloni M, Braga A, et al. Improved conversion efficiencies of thin-film silicon tandem (MICROMORPH™) photovoltaic modules. *Solar Energy Mater Solar Cells*. 2016;144:84-95. <https://doi.org/10.1016/j.solmat.2015.08.022>
63. Higuchi H, Negami T. Largest highly efficient 203 x 203 mm² CH₃NH₃PbI₃ perovskite solar modules. *Jpn J Appl Phys*. 2018;57:08RE11.
64. Hosoya M, Oooka H, Nakao H, Gotanda T, Mori S, Shida N, Hayase R, Nakano Y, Saito M. Organic thin film photovoltaic modules. Proceedings of the 93rd Annual Meeting of the Chemical Society of Japan 2013; 21-37.
65. Takamoto T. Application of InGaP/GaAs/InGaAs triple junction solar cells to space use and concentrator photovoltaic. 40th IEEE Photovoltaic Specialists Conference, Denver, June 2014.
66. Bheemreddy V, Liu BJJ, Wills A, Murcia CP. Life prediction model development for flexible photovoltaic modules using accelerated damp heat testing. IEEE 7th World Conf. on Photovoltaic Energy Conversion (WCPEC) 2018; 1249-1251.
67. Slade A, Garboushian V. 27.6% efficient silicon concentrator cell for mass production. Technical Digest, 15th International Photovoltaic Science and Engineering Conference, Shanghai, October 2005, 701.
68. Ward JS, Ramanathan K, Hasoon FS, et al. A 21.5% efficient Cu (In,Ga)Se₂ thin-film concentrator solar cell. *Prog Photovolt: Res Appl*. 2002;10(1):41-46.
69. Dimroth F, Tibbits TND, Niemeyer M, et al. Four-junction wafer-bonded concentrator solar cells. *IEEE J Photovolt*. 2016;6(1):343-349. <https://doi.org/10.1109/JPHOTOV.2015.2501729>
70. NREL. Press Release NR-4514, 16 December 2014.
71. Press Release, Sharp Corporation, 31 May 2012 (accessed at <http://sharp-world.com/corporate/news/120531.html> on 5 June 2013).
72. Jain N, Schulte KL, Geisz JF, et al. High-efficiency inverted metamorphic 1.7/1.1 eV GaInAsP/GaInAs dual-junction solar cells. *Appl. Phys. Lett*. 2018;112:053905.
73. Steiner M, Siefer G, Schmidt T, Wiesenfarth M, Dimroth F, Bett AW. 43% sunlight to electricity conversion efficiency using CPV. *IEEE J Photovolt*. 2016;6(4):1020-1024. <https://doi.org/10.1109/JPHOTOV.2016.2551460>
74. Green MA, Keevers MJ, Thomas I, Lasich JB, Emery K, King RR. 40% efficient sunlight to electricity conversion. *Prog Photovolt: Res Appl*. 2015;23(6):685-691.
75. Chiang CJ, Richards EH. A 20% efficient photovoltaic concentrator module. Conf. Record, 21st IEEE Photovoltaic Specialists Conference, Kissimmee, May 1990; 861-863.
76. <http://amonix.com/pressreleases/amonix-achieves-world-record-359-module-efficiency-rating-nrel-4> (accessed 23 October 2013).
77. van Riesen S, Neubauer M, Boos A, Rico MM, Gourdel C, Wanka S, Krause R, Guernard P, Gombert A. New module design with 4-junction solar cells for high efficiencies. Proceedings of the 11th Conference on Concentrator Photovoltaic Systems, 2015.
78. Martínez JF, Steiner M, Wiesenfarth M, Siefer G, Glunz SW, Dimroth F. Power rating procedure of hybrid CPV/PV bifacial modules. *Prog Photovolt Res Appl*. 2021;29(6):614-629.
79. Zhang F, Wenham SR, Green MA. Large area, concentrator buried contact solar cells. *IEEE Trans on Electron Devices*. 1995;42(1): 144-149.
80. Slooff LH, Bende EE, Burgers AR, et al. A luminescent solar concentrator with 7.1% power conversion efficiency. *Phys. Stat. Sol. (RRL)*. 2008;2(6):257-259.
81. Mülleijans H, Winter S, Green MA, Dunlop ED. What is the correct efficiency for terrestrial concentrator PV devices? 38th European Photovoltaic Solar Energy Conference, Sept. 2021 (accepted for presentation).
82. Gueymard CA, Myers D, Emery K. Proposed reference irradiance spectra for solar energy systems testing. *Solar Energy*. 2002;73(6): 443-467.

How to cite this article: Green MA, Dunlop ED, Hohl-Ebinger J, Yoshita M, Kopidakis N, Hao X. Solar cell efficiency tables (version 59). *Prog Photovolt Res Appl*. 2022;30(1):3-12. doi:10.1002/pip.3506

APPENDIX A

LIST OF DESIGNATED TEST CENTERS

A list of designated test centers is contained in an earlier issue.³ One address change:

Newport PV Lab.

3,050 North 300 West, North Logan, UT 8434, USA.

Contact: Geoffrey Wicks.

Lab: +1 406-556-2469 Office: +1 406-556-2489

Email: geoffrey.wicks@newport.com

(Terrestrial cells)